Pressure-enhanced C-H bond activation in chloromethane platinum(II) complexes

Dominik Schmitz, Marcel Kalter, Andrew C. Dunbar, Marcel Vöst, Andreas Fischer, Kilian Batke, Georg Eickerling, Klaus Ruhland, Jihaan Ebad-Allah, Christine A. Kuntscher, Wolfgang Scherer

Angaben zur Veröffentlichung / Publication details:

Schmitz, Dominik, Marcel Kalter, Andrew C. Dunbar, Marcel Vöst, Andreas Fischer, Kilian Batke, Georg Eickerling, et al. 2020. "Pressure-enhanced C-H bond activation in chloromethane platinum(II) complexes." *European Journal of Inorganic Chemistry* 2020 (1): 79–83. https://doi.org/10.1002/ejic.201901117.

ChemPubSoc Europe

DOI: 10.1002/ejic.201901117

EurJIC European Journal of Inorganic Chemistry

Communication

C–H Bond Activation

Pressure-Enhanced C–H Bond Activation in Chloromethane Platinum(II) Complexes

Dominik Schmitz,[a] Marcel Kalter,[a] Andrew C. Dunbar,[a] Marcel Vöst,[a] Andreas Fischer,[a] Kilian Batke,[a] Georg Eickerling,*[a] Klaus Ruhland,[a] Jihaan Ebad-Allah,[a,b] Christine Kuntscher,[a] and Wolfgang Scherer*[a]

Abstract: The nature of the interaction between chloromethanes $CH_{4-n}Cl_n$ and Pt(II) complexes has been studied by high-pressure X-ray diffraction and infrared spectroscopy in combination with DFT calculations. In case of electron rich complexes such as d^8-Pt(btz-*N*,*N*')(phenyl)*L* with *L* = phenyl, Cl, Br and btz = 2,2'-Bi-5,6-dihydro-4*H*-1,3-thiazine stable chloroform adducts with bridging hydrogen atoms in the η^1(C–H)Pt moieties were isolated which display highly activated C–H bonds. This activation is a consequence of a pronounced Pt(d_{z^2})→σ*(C–H) back donation and is signaled by large red-shifts of the isolated ν_{is}(C–H) stretching modes. The extent of the C–H bond activation and covalent Pt–H bond formation in the η^1(C–H)Pt moieties is thereby controlled by (*i*) the σ/π donor capabilities of the ligands *L*, (*ii*) the orientation of the coordinating C–H bond with regard to the Pt(d_{z^2}) orbital and (*iii*) the applied pressure.

The activation of carbon–hydrogen bonds is usually hampered by their rather apolar covalent character and large bond dissociation energies. For example the C–H bond dissociation enthalpies in simple alkanes such as methane [DH_{298} = 439.28(13) kJ mol^{-1}] are virtually as large as in the H_2 molecule [DH_{298} = 435.998(13) kJ mol^{-1}] displaying the prototype of a strong covalent bond.[1] As a consequence, alkanes are neither good electron donors nor good acceptors since the σ(C–H) bonding orbital is low in energy while the antibonding σ*(C–H) orbital is high lying. Hence, C–H bonds are generally considered to be chemically rather inert and their selective activation remains a challenge in organometallic chemistry.[2–4]

This obstacle can be overcome by metal-assisted C–H bond activation in cases where an alkane ligand coordinates either end-on (η^1) or side-on (η^2) to a metal-ligand fragment ML_n (Scheme 1).[5,6] In case of electron-rich late transition metal complexes two bonding scenarios with short *M*···H_{br}–C contacts are usually observed for methane and halomethane d^8-Pt complexes, where H_{br} denotes a bridging hydrogen atom. These are illustrated in case of the theoretical model systems $(CH_3)_2Pt(NH_3)(CH_4)$ **1a** and $(CH_3)_2Pt(NH_3)_2{\cdot}(CHCl_3)$ **1b** in Scheme 1. We note, that all DFT calculations were performed with ADF using the BP86 functional, the ZORA for the description of scalar relativistic effects, and the TZ2P basis set as implemented in ADF, see the Supporting Information (SI) for details. A density dependent dispersion correction was essential and applied in all cases.[7,8]

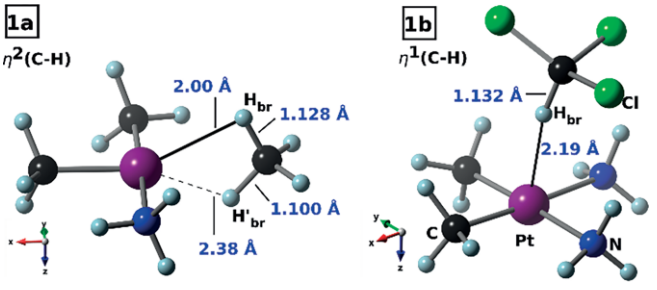

Scheme 1.

Compound **1a** represents the characteristic coordination geometry of σ methane complex. Similar η^2(C–H)Pt coordination modes are also predicted for intermediates in Shilov/Periana type catalytical oxidation reactions of methane.[3,9] Second order perturbation theory of natural bond orbitals (NBO)[10] suggests that the asymmetrical η^2(C–H)Pt coordination of the methane ligand [*r*(Pt···H_{br}) = 2.00 Å; *r*(Pt···C) = 2.60 Å] in **1a** is a consequence of the competing σ*(Pt–C)←σ (C–H) σ donation and Pt(d_{xz})→σ* (C–H) π back donation components. The resulting activation of the coordinating C–H_{br} bond is indicated by a distinct red-shift of the ν_{as}(C–H_{br}) stretching mode (2646 cm^{-1} in **1a**; 3072 cm^{-1} in CH_4) and a subtle C–H_{br} bond elongation of ca. 0.03 Å in comparison with free methane [*r*(C–H) = 1.096 Å]. However, an energy decomposition analysis (EDA)[11] reveals that the total bonding energy between the metal fragment and the methane ligand is rather small (20.0 kJ mol^{-1}). This is in line with recent low temperature-NMR studies in solution on

[a] *Institut für Physik, Universität Augsburg, Universitätsstr. 1, 86135 Augsburg, Germany*
E-mail: wolfgang.scherer@physik.uni-augsburg.de
[b] *Department of Physics, Tanta University, 31527 Tanta, Egypt*
Supporting information and ORCID(s) from the author(s) for this article are available on the WWW under https://doi.org/10.1002/ejic.201901117.

the Rh(I) complex $(PONOP)Rh(CH_4)^+$ [where PONOP is 2,6-(tBu$_2$PO)$_2$C$_5$H$_3$N and tBu is C(CH$_3$)$_3$].[12] These studies reveal that the coordination of the methane ligand to the metal is weak and the free energy of activation for methane dissociation is merely 60.7 kJ mol^{-1} at –87 °C. Despite the recent successes in isolating relatively stable σ alkane complexes in single crystals by solvent coordination[13] or via hydrogenation of transition metal olefin species via gas–solid reactions,[6] the trapping and isolation of σ-methane complexes remains a challenge.[12,14]

In contrast to **1a** the highly polar $C^{\delta-}$–$H^{\delta+}$ bond of the chloroform ligand prefers an axial coordination in $(CH_3)_2$Pt-$(NH_3)_2$•$(CHCl_3)$ **1b** by approaching the partially occupied Pt(d_{z^2}) orbital at the metal center and a short Pt···H_{br} distance of 2.186 Å. This suggests that the 16e *cis*-$(CH_3)_2Pt(NH_3)_2$ fragment can act as a nucleophile forming $Pt^{\delta+}$···$H^{\delta+}$–$C^{\delta-}$ metal hydrogen bonds.[15] However, the enormous red-shift of the isolated stretching mode, ν_{is}(C–H_{br}), by 570 cm^{-1} relative to uncoordinated $CHCl_3$ (3073 cm^{-1}) proposes a rather covalent bonding scenario. Indeed, second order perturbation theory NBO-analysis reveals that the Pt(d_{z^2})→σ*(C–H) back donation is complemented by additional Pt(RY)←σ(C–H) σ donation into unoccupied extravalent ("Rydberg") d orbitals at the metal.

A natural population analysis suggests that the Pt(RY)←σ(C–H) back donation is a consequence of the partial depopulation of the Pt(5d_{z^2}) orbital (1.78 e) in the *cis*-$(CH_3)_2Pt(NH_3)_2$ fragment. An EDA analysis shows that the absolute value of the orbital interaction energy between the chloroform ligand and the metal fragment in **1b** is surprisingly large (–85.8 kJ mol^{-1}) and comparable with that in the η^2(C–H)Pt σ methane complex **1a** (–72.8 kJ mol^{-1}). The charge density characteristics at the Pt···H_{br} bond critical point (BCP) also support a noticeable covalent Pt–H_{br} character in **1a** and **1b**. Accordingly, both model compounds display negative total energy densities $H(\mathbf{r})_c$ of –0.063 and –0.059 hartree Å^{-3} in combination with significant density accumulations $\rho(\mathbf{r})_c$ = 0.36 e Å^{-3} and 0.28 e Å^{-3} at the Pt···H_{br} BCPs, respectively. The corresponding delocalization indices, δ, of 0.24 (**1a**) and 0.21 (**1b**) are nearly as large as those in β-agostic benchmark systems of late transition metals such as $[EtNi(d^tbpe)]^+[BF_4]^-$ (d^tbpe = tBu$_2$PCH$_2$CH$_2$PtBu$_2$) with δ = 0.297.[17] Hence, **1b** might be considered as a η^1(C–H)Pt σ complex characterized by a predominant Pt(d_{z^2})→σ*(C–H) σ back donation component, while **1a** represents a highly asymmetric η^2(C–H)Pt σ complex with a strong Pt···H_{br} bond and a weak secondary Pt···H′$_{br}$ interaction. This is witnessed by the large r(Pt···H′$_{br}$) distance of 2.38 Å, a lacking Pt···H′$_{br}$ BCP, and a small delocalization index of δ = 0.12, respectively.

In the following we have inspected the potential energy surface of η^1(C–H)Pt moieties experimentally by high-pressure X-ray diffraction and infrared spectroscopy studies to gain further insight into the control parameters of the C–H activation process and the unusual bonding in square-pyramidal d^8-Pt chloroform complexes. The experimental model system d^8-Pt(btz-*N*,*N*′)-$(phenyl)_2$•$(CHCl_3)$ (**2**) which has first been isolated by Bruno et al.[18] marked the starting point of this systematic study (Figure 1a). **2** displays a short r(Pt···H_{br}) distance of 2.315 [2.332] Å and a Pt···H_{br} bond critical point of 0.20 e Å^{-3} in the theoretical electron density distribution obtained by DFT which is slightly smaller than in model system **1b** (see above). Note, that theoretical values will be specified in square brackets in the following, when compared with experimental data. The ∠Pt,H_{br},C angle of 176.8° [171.6°] in **2** hints for predominant Pt(d_{z^2})→σ*(C–H) back donation which provides the major electronic stabilization of the chloroform coordination as in model **1b**.

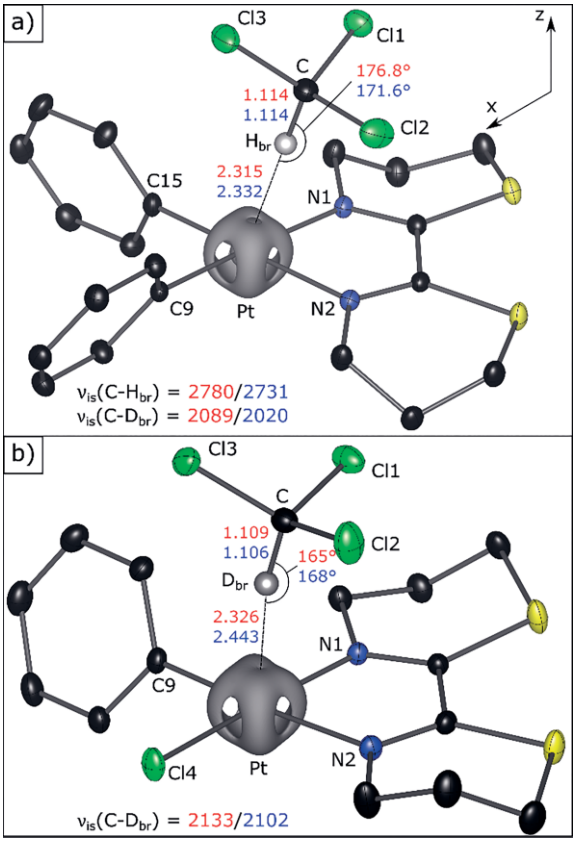

Figure 1. Structural models of **2** and **4** at ambient pressure by X-ray diffraction studies at 100 K (50 % ellipsoids). Hydrogen atoms at the phenyl and btz ligands are omitted for clarity reasons. Salient bond lengths (ref 16) are given in Å, ν_{is}(C–H_{br}) and ν_{is}(C–D_{br}) stretching modes are given in cm^{-1}. Experimental and theoretical values are specified in red and blue color, respectively. The ELF envelope maps [η(**r**) = 0.61] as obtained from DFT calculations are shown at the platinum atoms.

We note, that the metal-ligand interaction in **2** has been originally classified as purely electrostatic in terms of a metal hydrogen bond.[19] According to Thakur et al. complexes forming $Pt^{\delta+}$···$H_{br}{}^{\delta+}$–$C^{\delta-}$ metal hydrogen bonds are usually characterized by a non-activated or even shortened r(C–H_{br}) distance.[19] However, inspection of the IR data clearly reveals that the η^1(C–H)Pt unit of **2** displays – like our model system **1b** – a highly activated C–H_{br} bond as reflected by an isolated ν_{is}(C–H_{br}) stretching mode of 2780 cm^{-1} which is significantly red-shifted with respect to the free chloroform ligand [ν_{is}(C–H) = 3034 cm^{-1}] in the gas phase.[20] We can also rule out that the observed C–H bond activation in **2** is merely a consequence of the crystal packing since molecular DFT calculations reproduce virtually the same structural parameters for the η^1(C–H)Pt moiety and also the distinct red-shift of the corresponding ν_{is}(C–H_{br}) stretching mode, i.e. [2731 cm^{-1}] in **2** and [3086 cm^{-1}] in non-coordinated $CHCl_3$ (Figure 1a). Utilizing

McKean's empirical correlation,[21,22] which links *r*(C–H) bond lengths to isolated ν_{is}(C–H) stretching frequencies, the red shift of ν_{is}(C–H_{br}) is connected to a small but significant C–H_{br} bond activation in the η^1(C–H)Pt moieties of **2** {*r*(C–H_{br}) = 1.114 [1.114] Å} relative to free $CHCl_3$ {*r*(C–H) = 1.080(2)[23] [1.090] Å}. Hence, the metal-induced C–H_{br} bond elongation in **2** is ca. 0.034 Å [0.024 Å] and accompanied by a significant red-sift of ν_{is}(C–H_{br}) by ca. 254 cm^{-1} which compares well with those observed in transition metal alkyls displaying pronounced agostic interactions.[24] Rather clear evidence for the covalent character of the η^1(C–H)Pt moieties emerges from a distinct band broadening of the ν_{is}(C–H_{br}) stretching modes in the IR pattern of **2** (Figure 2). This characteristic feature also provides clear evidence for the bridging character of the coordinating hydrogen atoms within the partially covalent η^1(C–H)Pt moieties in **2**.[25,26]

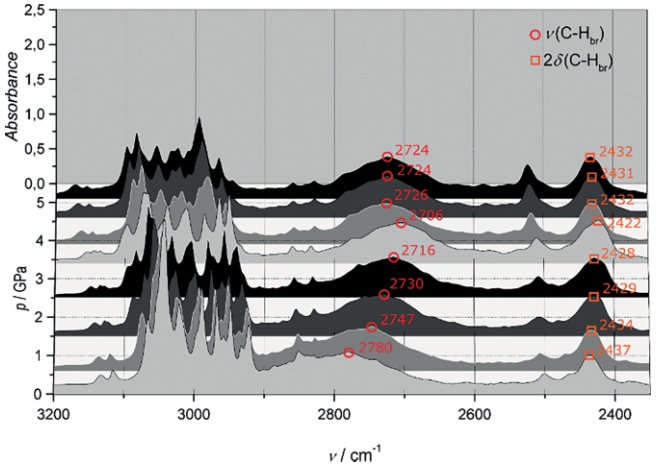

Figure 2. Pressure-dependency of the ν_{is}(C–H_{br}) stretching mode and the first overtone of the δ(C–H_{br}) deformation mode of the coordinating chloroform ligand in **2**. Only the ν_{is}(C–H_{br}) and the δ(C–H_{br}) modes of the η^1(C–H)Pt units show a distinct red-shift up to 3.4(1) GPa due to the activation of the metal-coordinating (C–H_{br}) bond. In contrast, all remaining ν_{is}(C–H) stretching modes in **2** are blue-shifted and compressed upon increasing the hydrostatic pressure.

The electronic motivation to form a stable chloroform complex is stressed by the finding that **2** can accommodate a second coordinating $CHCl_3$ molecule yielding the complex Pt(btz-*N*,*N*′)$(C_6H_5)_2(CHCl_3)_2$ (**2a**; see the Supporting Information for experimental data). Both chloroform ligands in **2a** compete electronically via the Pt(d_{z^2})→σ^*(C–H) back donation mechanism for the same density accumulation at the metal. As a result, the calculated *r*(Pt···H_{br}) distances of 2.356 Å and 2.363 Å in **2a** are somewhat larger than in **2** (2.332 Å). Even longer *r*(Pt···H_{br}) distances of 2.397 Å and 2.443 Å were calculated for Pt(btz-*N*,*N*′)$(C_6H_5)(X)(CDCl_3)$ {*X* = Br (**3**) and Cl (**4**)}, respectively. **3** and **4** can be derived from **2** by the replacement of one of the phenyl ligands at the Pt atom by an electron withdrawing bromo or chloro substituent. DFT studies predict that the C–H bond activation decreases with increasing electronegative character of the substituents at the metal atom: *r*(C–H_{br}) = 1.114 Å (**2**) > 1.107 Å (**3**) > 1.106 Å (**4**). This trend is in line with the experimentally observed blue shift of the corresponding ν_{is}(C–D_{br}) stretching modes when one phenyl group in **2** [ν_{is}(C–D_{br}) = 2089 cm^{-1}] is replaced by a bromo or chloro ligand: ν_{is}(C–D_{br}) = 2139 cm^{-1} and 2133 cm^{-1} in **3** and **4**, respectively.[20] Accordingly, the diminished C–H_{br} bond activation in **3** and **4** might be taken as direct evidence for a reduced Pt(d_{z^2})→σ^*(C–H) back donation as a consequence of the electron withdrawing character of the halogen ligand at the platinum atom. In case of model system **1b** substitution of one methyl group by a chloro ligand also leads to a weakening of the Pt···H_{br}–C interaction (Pt···H_{br} = 2.276 Å). The Pt(d_{z^2})→σ^*(C–H) back donation is further controlled by the polarity of the $H^{\delta+}$–$C^{\delta-}$ bond of the respective chloromethane ligand. A reduced C–H polarity weakens the Pt(d_{z^2})→σ^*(C–H) back donation in line with increasing Pt–H_{br} bond lengths in the series $(CH_3)_2Pt(NH_3)_2$•$(CH_{4-n}Cl_n)$: 2.186 Å (*n* = 3) < 2.294 Å (*n* = 2) < 2.466 Å (*n* = 1) < 2.838 Å (*n* = 0).

This electronic trend in the series $(CH_3)_2Pt(NH_3)_2$•$(CH_{4-n}Cl_n)$ as well as in the experimental models **2, 3** and **4** is, however, reversed in case of η^2(C–H)Pt σ complexes with a predominant Pt←σ(C–H) σ donation component such as model system **1a**. Early theoretical studies by Cundari[27] showed that in case of the related square planar model systems $Ir(PH_3)_2X(\eta^1\text{-}CH_4)$ [*X* = H (**5a**), Cl (**5b**)] the C–H bond activation increases in contrast to **2**, **3** and **4** when *X* represents an electron withdrawing ligand. Hence, η^1(C–H)Pt σ complexes with predominant Pt(d)→σ^*(C–H) back donation (**1b**, **2**, **2a**, **3**, **4**) should be discriminated from η^2(C–H)Pt complexes (**1a**, **5a**, **5b**) where the Pt←σ(C–H) σ donation component prevails.

To provide further evidence, that **2**, **2a**, **3** and **4** should be classified as η^1-σ alkane complexes we analyzed their potential energy surface (PES) by high-pressure studies. This methodology has been introduced recently by one of us to study the related bonding scenario of σ agostic interactions and σ silane complexes.[28a,29] We will show in the following that application of hydrostatic pressure can also be used to compress the η^1(C–H)Pt moieties in single crystals of **2** to push the C–H_{br} bond of the chloroform ligand closer to the metal. As a consequence we might systematically enhance the Pt(d_{z^2})→σ*(C–H) back donation and Pt(RY)←σ(C–H) σ donation to trigger the C–H bond activation upon increasing pressure similar to the electronic situation in σ-agostic d^8 Ni complexes.[28] This pressure-induced C–H bond activation is accomplished by placing single crystals of **2** in a diamond anvil cell while the structural and electronic changes are observed in-situ by X-ray diffraction and IR studies. A mixture of *n*-pentane/isopentane was used as pressure-transmitting medium for the diffraction experiments and liquid nitrogen for the corresponding IR studies.

Figure 2 depicts the observed pressure-dependency of the ν_{is}(C–H_{br}) stretching modes of the η^1(C–H)Pt moiety of **2** which clearly signals an increasing softening of the C–H_{br} bond of the chloroform ligand with increasing pressure [ν_{is}(C–H_{br}) = 2780 cm^{-1} at 0 GPa and ν_{is}(C–H_{br}) = 2706 cm^{-1} at 3.4(1) GPa]. Using again McKean's empirical correlation we can relate the ν_{is}(C–H_{br}) red shift of 74 cm^{-1} [90 cm^{-1} @ 4.0 GPa] with a pressure-induced activation of the coordinating C–H bond.[21,22] This yields an activated *r*(C–H_{br}) bond length of approx. 1.121 Å in **2** at 3.4(1) GPa which is nearly 4.1 pm larger than the non-activated *r*(C–H) bond in free chloroform and nearly as large as the agostic *r*(C–H) bond length (1.13 Å) in $EtTiCl_3$(dmpe)[30]

representing the textbook example of an agostic transition metal alkyl complex.

In the next step of our analysis we tried to clarify whether the pressure-induced C–H bond activation in **2** is connected with a stronger interaction between the bridging C–H bond of the chloroform ligand and the Pt(d_{z^2}) orbital. Figure 3a provides an overlay of the individual structures of **2** at 0.0 and 2.6(1) GPa. In this pressure regime the C–H_{br} bond activation is correlated with a virtually linear shift of the chloroform ligand along the Pt•••H_{br} vector. The observed shortening of the *r*(Pt•••H_{br}) distance by ca. 0.25 Å [0.13 Å @ 2.0 GPa] significantly enhances the overlap between the Pt(d_{z^2}) and the σ/σ*(C–H) orbitals which span two 3c2e orbitals of bonding and non-bonding character, respectively.

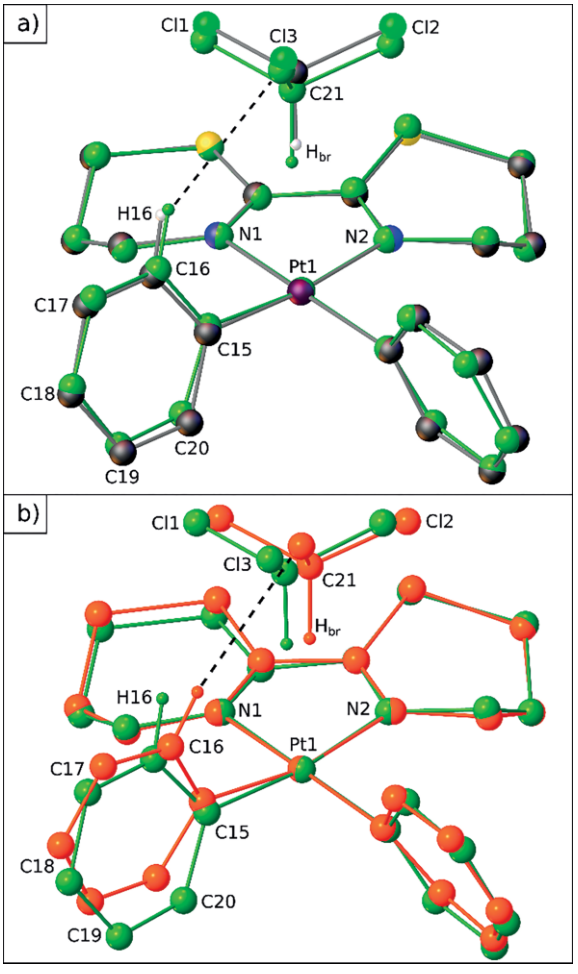

Figure 3. Overlay of the ball and stick models of **2** obtained by experimental X-ray diffraction studies using a diamond anvil cell (DAC) at 2.6(1) GPa (green) with the structure models at a) ambient pressure (ca. 0.0 GPa) and b) 3.9(1) GPa (orange).

The structural changes above 2.6(1) GPa, however, reduce the Pt(d_{z^2})•••H_{br}–C interaction – in line with the observed blue-shift of the ν_{is}(C–H_{br}) bands (Figure 2). Figure 3b depicts the corresponding structural changes between 2.6(1) and 3.9(1) GPa.

Detailed charge density analyses of Hirshfeld-surfaces[31] reveal that pressure-induced *intermolecular* interactions between the btz ligand and one of the phenyl rings enforce an out-of-plane rotation of the latter (Figure 3b) at elevated pressures (SI). As a consequence of this out-of-plane rotation the *intramolecular* repulsion between the phenyl H16 atom and one of the chlorine substituents of the coordinating chloroform ligand (SI) increases. At pressures above 3.4(1) GPa this results in a distinct shift of the coordinating chloroform ligand away from the axial lobes of the Pt(d_{z^2}) orbital. Thus, the donor–acceptor interactions become reduced at pressures above 3.4(1) GPa by the decreased overlap of the Pt(d_{z^2}) atomic orbital with the σ/σ*(C–H) orbitals. Hence, our high-pressure study allowed us to study the potential energy surface of **2** by mapping the structural and electronic changes upon shifting the coordinating C–H_{br} bond either approximately parallel (in *z*-direction) or perpendicular to the lobes of the Pt(d_{z^2}) orbital.

The strict dependency of the C–H_{br} bond activation on the overlap angle between the Pt(d_{z^2}) and the σ/σ*(C–H) orbitals clearly supports the presence of a covalent η^1(C–H)Pt moiety. This finding is further in line with the pronounced broadening of the isolated ν_{is}(C–H_{br}) stretching modes in the infrared studies. In case of agostic interactions and the related σ silane complexes[24,32] we have shown that the presence of local Lewis acidic sites at the transition metal center *M* provides a necessary prerequisite for the establishment of covalent *M*•••H_{br}–C interactions. This is actually also the case for the Pt•••H_{br}–C interactions in **2**, **2a**, **3** and **4**. In all three cases the bridging C–H bonds of the choroform ligands point to a center of charge depletion in the valence density of the platinum atom signaling the partial depopulation of the natural Pt($5d_{z^2}$)-type orbitals in the metal ligand fragments (Figure 1).

These depletion sites are also revealed by minima in the electron localization function (ELF)[33,34] at the platinum atom along the local *z*-axis (Figure 1). The extent of these depletion sites appears to be directly connected with the strength of the Pt•••H_{br}–C interaction and thus decreases in Pt(btz-*N*,*N*′)(C_6H_5)-(*X*)($CDCl_3$) with increasing electron-withdrawing character of *X*: *X* = Phenyl (**2**) > Br (**3**) > Cl (**4**).

To conclude, combined high-pressure X-ray and infrared studies allowed for the first time to study a pressure-enhanced C–H bond activation in an organometallic complex. The d^8 platinum complexes **2**, **2a**, **3** and **4** employed in this study could be characterized as σ complexes displaying η^1(C–H)Pt moieties.

Experimental Section

Complexes **2–4** were synthesized according to modified literature methods (see ref 18 and the SI). The high-pressure single crystal diffraction experiments of **2** were conducted with a Merrill Bassett DAC with 0.6 mm culet conical diamond anvils. A crystal was placed into a pre-indented stainless steel gasket and surrounded by a 1:1 mixture of *n*-pentane and isopentane acting as pressure-transmitting medium. Details of the X-ray diffraction experiments at high pressures (**2**) and at low temperatures (**2–4**) are given in the SI. Pressure-dependent transmittance measurements were conducted in the frequency range of 550–8000 cm^{-1} using a Bruker IRscope II coupled to a Bruker IFS 66v/s FT-IR spectrometer. A *Diacell* Cryo-DAC-Mega with type IIa diamonds was used with a pre-indented CuBe gasket and nitrogen as hydrostatic pressure-transmitting me-

dium. The periodic B3LYP DFT calculations at various pressures used the CRYSTAL09 code; see the SI for further details.

CCDC 1926196 (for **2**), 1926197 (for **2a**), 1926198 (for **3**), 1926199 (for **4**), and 1926200–1926204 (for **2** at high pressure) contain the supplementary crystallographic data for this paper. These data can be obtained free of charge from The Cambridge Crystallographic Data Centre.

Acknowledgments

This work was supported by the DFG (SPP1178) project number SCHE478/12-1

Keywords: Bond activation · σ-Complexes · Platinum · Charge density · Density functional calculations

[1] S. J. Blanksby, G. B. Ellison, *Acc. Chem. Res.* **2003**, *36*, 255–263.
[2] B. A. Arndtsen, R. G. Bergman, T. A. Mobley, T. H. Peterson, *Acc. Chem. Res.* **1995**, *28*, 154–162.
[3] H. Heiberg, L. Johansson, O. Gropen, O. B. Ryan, O. Swang, M. Tilset, *J. Am. Chem. Soc.* **2000**, *122*, 10831–10845.
[4] a) S. Feyel, J. Döbler, D. Schröder, J. Sauer, H. Schwarz, *Angew. Chem. Int. Ed.* **2006**, *45*, 4681–4685; *Angew. Chem.* **2006**, *118*, 4797–4801; b) V. N. Cavaliere, D. J. Mindiola, *Chem. Sci.* **2012**, *3*, 3356–3365; c) N. J. Gunsalus, A. Koppaka, S. H. Park, S. M. Bischof, B. G. Hashiguchi, R. A. Periana, *Chem. Rev.* **2017**, *117*, 8521–8573; d) P. Gandeepan, T. Müller, D. Zell, G. Cera, S. Warratz, L. Ackermann, *Chem. Rev.* **2019**, *119*, 2192–2452.
[5] C. Hall, R. N. Perutz, *Chem. Rev.* **1996**, *96*, 3125–3146.
[6] a) S. D. Pike, A. L. Thompson, A. G. Algarra, D. C. Apperley, S. A. Macgregor, A. S. Weller, *Science* **2012**, *337*, 1648–1651; b) S. D. Pike, F. M. Chadwick, N. H. Rees, M. P. Scott, A. S. Weller, T. Krämer, S. A. Macgregor, *J. Am. Chem. Soc.* **2015**, *137*, 820–833; c) A. S. Weller, F. M. Chadwick, A. I. McKay, in *Adv. Organomet. Chem* (Ed.: P. J. Pérez), Academic Press, **2016**, pp. 223–276; d) A. J. Martínez-Martínez, B. E. Tegner, A. I. McKay, A. J. Bukvic, N. H. Rees, G. J. Tizzard, S. J. Coles, M. R. Warren, S. A. Macgregor, A. S. Weller, *J. Am. Chem. Soc.* **2018**, *140*, 14958–14970.
[7] Q. Lu, F. Neese, G. Bistoni, *Phys. Chem. Chem. Phys.* **2019**, *21*, 11569–11577.
[8] S. N. Steinmann, C. Corminboeuf, *J. Chem. Theory Comput.* **2011**, *7*, 3567–3577.
[9] J. Kua, X. Xu, R. A. Periana, W. A. Goddard, *Organometallics* **2002**, *21*, 511–525.
[10] C. R. Landis, F. Weinhold, in *The Chemical Bond: Fundamental Aspects of Chemical Bonding*, John Wiley & Sons, Ltd, **2014**, pp. 91–120.
[11] F. M. Bickelhaupt, E. Baerends, *Rev. Comput. Chem.* **2000**, *15*, 1–86.
[12] W. H. Bernskoetter, C. K. Schauer, K. I. Goldberg, M. Brookhart, *Science* **2009**, *326*, 553–556.
[13] a) D. R. Evans, T. Drovetskaya, R. Bau, C. A. Reed, P. D. W. Boyd, *J. Am. Chem. Soc.* **1997**, *119*, 3633–3634; b) I. Castro-Rodriguez, H. Nakai, P. Gantzel, L. N. Zakharov, A. L. Rheingold, K. Meyer, *J. Am. Chem. Soc.* **2003**, *125*, 15734–15735; c) E. D. Bloch, W. L. Queen, R. Krishna, J. M. Zadrozny, C. M. Brown, J. R. Long, *Science* **2012**, *335*, 1606–1610.
[14] a) G. E. Ball, C. M. Brookes, A. J. Cowan, T. A. Darwish, M. W. George, H. K. Kawanami, P. Portius, J. P. Rourke, *Proc. Natl. Acad. Sci. USA* **2007**, *104*, 6927–6931; b) J. Campos, S. Kundu, D. R. Pahls, M. Brookhart, E. Carmona, T. R. Cundari, *J. Am. Chem. Soc.* **2013**, *135*, 1217–1220; c) O. Torres, J. A. Calladine, S. B. Duckett, M. W. George, R. N. Perutz, *Chem. Sci.* **2015**, *6*, 418–424; d) B. Chan, G. E. Ball, *J. Chem. Theory Comput.* **2013**, *9*, 2199–2208.
[15] L. Brammer, *Dalton Trans.* **2003**, 3145–3157.
[16] The r(C–H_{br}) and r(C–D_{br}) distances in the refinements of the X-ray diffraction data were derived from the experimental ν_{is}(C–H_{br}) and ν_{is}(C–D_{br}) stretching modes using McKean's empirical correlation (ref 21 and 22).
[17] W. Scherer, V. Herz, A. Brück, C. Hauf, F. Reiner, S. Altmannshofer, D. Leusser, D. Stalke, *Angew. Chem. Int. Ed.* **2011**, *50*, 2845–2849; *Angew. Chem.* **2011**, *123*, 2897–2902.
[18] G. Bruno, S. Lanza, F. Nicolo, *Acta Crystallogr., Sect. C* **1990**, *46*, 765–767.
[19] T. S. Thakur, G. R. Desiraju, *THEOCHEM* **2007**, *810*, 143–154.
[20] A. Kimoto, H. Yamada, *Bull. Chem. Soc. Jpn.* **1968**, *41*, 1096–1104.
[21] D. C. McKean, *Chem. Soc. Rev.* **1978**, *7*, 399–422.
[22] D. C. McKean, *J. Mol. Struct.* **1984**, *113*, 251–266.
[23] J.-M. Colmont, D. Priem, P. Dréan, J. Demaison, J. E. Boggs, *J. Mol. Spectrosc.* **1998**, *191*, 158–175.
[24] W. Scherer, G. S. McGrady, *Angew. Chem. Int. Ed.* **2004**, *43*, 1782–1806; *Angew. Chem.* **2004**, *116*, 1816–1842.
[25] M. A. Andrews, S. W. Kirtley, H. D. Kaesz, in *Transit. Met. Hydrides*, American Chemical Society, **1978**, pp. 215–231.
[26] D. L. M. Suess, J. C. Peters, *J. Am. Chem. Soc.* **2013**, *135*, 4938–4941.
[27] T. R. Cundari, *J. Am. Chem. Soc.* **1994**, *116*, 340–347.
[28] a) W. Scherer, A. C. Dunbar, J. E. Barquera-Lozada, D. Schmitz, G. Eickerling, D. Kratzert, D. Stalke, A. Lanza, P. Macchi, N. P. M. Casati, J. Ebad-Allah, Ch. Kuntscher, *Angew. Chem. Int. Ed.* **2015**, *54*, 2505–2509; *Angew. Chem.* **2015**, *127*, 2535–2539; b) M. P. Mitoraj, M. G. Babashkina, K. Robeyns, F. Sagan, D. W. Szczepanik, Y. V. Seredina, Y. Garcia, D. A. Safin, *Organometallics* **2019**, *38*, 1973–1981.
[29] P. Meixner, K. Batke, A. Fischer, D. Schmitz, G. Eickerling, M. Kalter, K. Ruhland, K. Eichele, J. E. Barquera-Lozada, N. P. M. Casati, et al., *J. Phys. Chem. A* **2017**, *121*, 7219–7235.
[30] D. C. McKean, G. Sean McGrady, A. J. Downs, W. Scherer, A. Haaland, *Phys. Chem. Chem. Phys.* **2001**, *3*, 2781–2794.
[31] M. A. Spackman, D. Jayatilaka, *CrystEngComm* **2009**, *11*, 19–32.
[32] W. Scherer, P. Meixner, J. E. Barquera-Lozada, C. Hauf, A. Obenhuber, A. Brück, D. J. Wolstenholme, K. Ruhland, D. Leusser, D. Stalke, *Angew. Chem. Int. Ed.* **2013**, *52*, 6092–6096; *Angew. Chem.* **2013**, *125*, 6208–6212.
[33] A. D. Becke, K. E. Edgecombe, *J. Chem. Phys.* **1990**, *92*, 5397–5403.
[34] B. Silvi, A. Savin, *Nature* **1994**, *371*, 683–686.

Received: October 17, 2019